

UNCLASSIFIED

AD 401 339

*Reproduced
by the*

DEFENSE DOCUMENTATION CENTER

FOR

SCIENTIFIC AND TECHNICAL INFORMATION

CAMERON STATION ALEXANDRIA, VIRGINIA



UNCLASSIFIED

NOTICE: When government or other drawings, specifications or other data are used for any purpose other than in connection with a definitely related government procurement operation, the U. S. Government thereby incurs no responsibility, nor any obligation whatsoever; and the fact that the Government may have formulated, furnished, or in any way supplied the said drawings, specifications, or other data is not to be regarded by implication or otherwise as in any manner licensing the holder or any other person or corporation, or conveying any rights or permission to manufacture, use or sell any patented invention that may in any way be related thereto.

63-3-2

MEMORANDUM
RM-3000-PR
MARCH 1963

401 339

CATALOGED BY ASTIA
AS AD NO. 401339

HYPERSONIC STRONG VISCOUS
INTERACTION ON A FLAT PLATE WITH
SURFACE MASS TRANSFER

Ting-Yi Li and Joseph F. Gross



PREPARED FOR:
UNITED STATES AIR FORCE PROJECT RAND

The RAND Corporation
SANTA MONICA • CALIFORNIA

MEMORANDUM
RM-3000-PR
MARCH 1963

**HYPersonic STRONG VISCOUS
INTERACTION ON A FLAT PLATE WITH
SURFACE MASS TRANSFER**

Ting-Yi Li and Joseph F. Gross

This research is sponsored by the United States Air Force under Project RAND—contract No. AF 49(638)-700 monitored by the Directorate of Development Planning, Deputy Chief of Staff, Research and Development, Hq USAF. Views or conclusions contained in this Memorandum should not be interpreted as representing the official opinion or policy of the United States Air Force.

The **RAND** *Corporation*

1700 MAIN ST • SANTA MONICA • CALIFORNIA

PREFACE

Advances in the design of hypersonic vehicles can be realized only if the structural and thermal problems engendered by the high surface-heating rates are alleviated. The injection of a coolant into the boundary layer on the surface of a vehicle, i.e., mass-transfer cooling, is one method for reducing heating rates.

In this Memorandum the problem of a hypersonic flow on a flat plate with surface mass transfer is examined to determine the significant parameters which affect the solution. This work is the beginning of a general study of hypersonic flow with mass-transfer cooling.

SUMMARY

An account is presented of the development of an approximation theory for the problem of hypersonic strong viscous interaction on a flat plate with mass transfer at the plate surface. The disturbance-flow region is divided into inviscid- and viscous-flow regions. The hypersonic-small-perturbation theory is applied to the solution of the inviscid-flow region. The method of similar solutions of compressible laminar-boundary-layer equations is applied to the treatment of the viscous-flow region. The pressure and the normal velocity are matched between the inviscid- and viscous-flow solutions. The law of surface mass transfer for similar solutions is derived. Formulas for induced surface pressure, boundary-layer thickness, skin-friction coefficient, and heat-transfer coefficient are obtained. Numerical results and their significance are discussed.

The most significant results obtained from the data presented are (1) the boundary layer thickens with injection so that the interaction phenomena increase, (2) the skin-friction coefficient and heat-transfer coefficient exhibit remarkably linear behavior with respect to injection, and (3) the Reynolds Analogy is valid only for the cold-wall case.

CONTENTS

PREFACE.....	111
SUMMARY.....	v
LIST OF SYMBOLS.....	ix
Section	
I. INTRODUCTION.....	1
II. BASIC EQUATIONS AND BOUNDARY CONDITIONS.....	4
III. THE INVISCID-FLOW REGION.....	8
IV. THE VISCOUS-FLOW REGION.....	15
V. THE LAW OF SURFACE MASS TRANSFER FOR SIMILAR SOLUTIONS	24
VI. MATCHING OF THE INVISCID- AND VISCOUS-FLOW SOLUTIONS..	26
VII. RESULTS AND DISCUSSION.....	31
Boundary-Layer Thickness.....	31
Induced Surface Pressure.....	31
Velocity Profiles.....	34
Temperature Profiles.....	38
Skin-Friction Coefficient.....	42
Heat-Transfer Coefficient.....	42
VIII. CONCLUDING REMARKS.....	46
REFERENCES.....	49

SYMBOLS

- c_f = local skin-friction coefficient
- c_h = local dimensionless heat-transfer coefficient (Stanton number)
- c_p = specific heat at constant pressure
- f = inviscid similarity function defined in Eq. (22)
- H = specific total enthalpy
- i = specific thermodynamic enthalpy
- K_g = hypersonic similarity parameter defined in Eq. (17)
- $K_o = K(o)$ = injection parameter
- k = thermal conductivity
- L = characteristic length
- M = Mach number
- n = exponent defined in Eq. (20)
- Pr = Prandtl number
- p = pressure
- R = universal gas constant
- s = specific entropy
- T = temperature, $c_p \mu / k$
- U = free-stream velocity in x-direction
- u = velocity in x-direction
- v = velocity in y-direction
- x = distance in direction parallel to plate surface
- y = distance in direction normal to plate surface
- $\beta = \frac{\gamma - 1}{\gamma}$
- γ = ratio of specific heats, c_p / c_v
- ϵ = parameter defined in Eq. (12)
- η = similarity variable for boundary layer

- θ = inviscid similarity parameter defined in Eq. (21)
- μ = viscosity
- ν = kinetic viscosity, μ/ρ
- ρ = density
- τ = surface shearing stress
- ψ = stream function in inviscid flow region
- $\bar{\psi}$ = conventional stream function in viscous region
- ω = see Eq. (1)

Subscript

- δ = edge of boundary layer
- $*$ = nondimensional
- s = shock
- l = free stream
- w = wall
- o = stagnation

I. INTRODUCTION

Alleviation of aerodynamic heating on the surface of a hypersonic-velocity vehicle can be achieved by cooling methods using surface mass transfer. Three such methods that hold great promise are⁽¹⁾

1. Transpiration cooling
2. Film cooling
3. Sublimation or ablation cooling

In the transpiration-cooling method, the surface-mass-transfer rate is arbitrarily controlled. In the methods of film cooling and sublimation or ablation cooling, the surface-mass-transfer rate is not entirely arbitrary. However, all of these methods possess the same main feature: the injection of a foreign material from the body surface into the boundary layer. As a result of this injection, it can be expected that several new elements must be admitted into the analysis of the boundary-layer phenomena:

1. The heat-energy balance in the boundary layer must be considerably modified to account for the surface-mass-transfer effects.
2. The momentum equation is modified to include the normal velocity component at the wall. This results in a change in the velocity distribution in the boundary layer.
3. The injected foreign material will diffuse through the main boundary-layer stream, causing a change in the composition of the fluid.

Surely these effects are mutually interdependent. An accurate analytic formulation of the multicomponent-boundary-layer flow is possible

but difficult. As a simple approximation, the problem can be treated as the laminar-boundary-layer flow of a binary mixture.⁽²⁾ Adopting the simplifying assumption that the Lewis number is unity, the analytical characteristics of the laminar-boundary-layer equations for a binary mixture have been examined in Ref. 3, where the introduction of a new characteristic-temperature function reduces the binary-boundary-layer equations to those for a pure gas. Therefore, an approximate analysis of the surface-mass-transfer effects can be made by considering only those modifications mentioned in items 1 and 2 above. By interpretation of these initial results according to the method of Ref. 3, estimates of the effects due to item 3 above can be obtained. In the main part of this Memorandum, therefore, we shall deal with the boundary-layer equations of a pure gas.

It is well known in the study of hypersonic viscous flow past a flat plate that there exists a region of strong interaction between the leading-edge shock wave and the viscous boundary layer. In the present Memorandum, we shall study the effects of surface mass transfer on this strong-interaction phenomena. This problem has previously been treated by Yasuhara,⁽⁴⁾ who confined his attention to the case of an insulated flat plate and used the Karman-Pohlhausen method for solution of the equations. For the surface-mass-transfer rates used in Ref. 4, we shall show that the boundary-layer equations admit similar solutions. We shall then proceed to apply the method of similar solutions of the compressible-laminar-boundary-layer equations⁽⁵⁾ to the present problem. Both the insulated and the noninsulated flat plates will be considered. In deriving the system of differential

equations, we shall neglect terms of the order of $1/M_1^2$ where the free-stream Mach number is assumed to be $M_1 \gg 1$. The differential equations thus obtained are nonlinear and can be integrated numerically. Results of such integration (for $Pr = 1$, $\omega = 1$) will be presented. These results will then be used to provide estimates of the effects of mass transfer on the strong-interaction phenomena. We shall find that the magnitude of the surface temperature plays an important role in this problem. Indeed, one effect of injection is to keep the plate surface temperature low, which tends to alleviate the strong-interaction phenomena. Another effect of injection is to increase the boundary-layer displacement thickness and thus to increase the strong-interaction phenomena. These opposing effects are both important for a certain range of injection rates. In the numerical examples, we shall also consider some cases of negative injection rates which can be interpreted as applying suction at the body surface.

II. BASIC EQUATIONS AND BOUNDARY CONDITIONS

Consider a flat plate at $y = 0$ (Fig. 1) and extending from $x = 0$ to $x = \infty$. At the plate surface, a particular rate of mass transfer due to injection is allowed, the rate of mass transfer being determined in a manner to be described later. A uniform stream with velocity U parallel to the plate is deflected by the viscous boundary layer on the plate surface. This flow deflection is accompanied by a shock wave emanating from the leading edge of the plate. There is a nonlinear coupling between the growth of the boundary layer and the variation of the shock-wave strength in the strong-interaction region on the flat plate where

$$\frac{M_1^{2\omega} v_1}{U} \ll x \ll \frac{M_1^k + 2\omega v_1}{U} \quad (1)$$

x being the distance from the leading edge of the plate. The disturbed flow is separated from the undisturbed flow by the leading-edge shock wave. The region between the shock wave and the plate surface can be divided in the range of x , as defined in Eq. (1), into an inviscid-flow region and a viscous-boundary-layer region. (6, 7) The basic system of equations for the disturbed-flow region can be written as follows:

$$\frac{\partial}{\partial x}(\rho u) + \frac{\partial}{\partial y}(\rho v) = 0 \quad (2)$$

$$\rho u \frac{\partial u}{\partial x} + \rho v \frac{\partial u}{\partial y} = -\frac{\partial p}{\partial x} + \frac{\partial}{\partial y} \left(\mu \frac{\partial u}{\partial y} \right) \quad (3)$$

$$\rho u \frac{\partial v}{\partial x} + \rho v \frac{\partial v}{\partial y} = -\frac{\partial p}{\partial y} \quad (4)$$

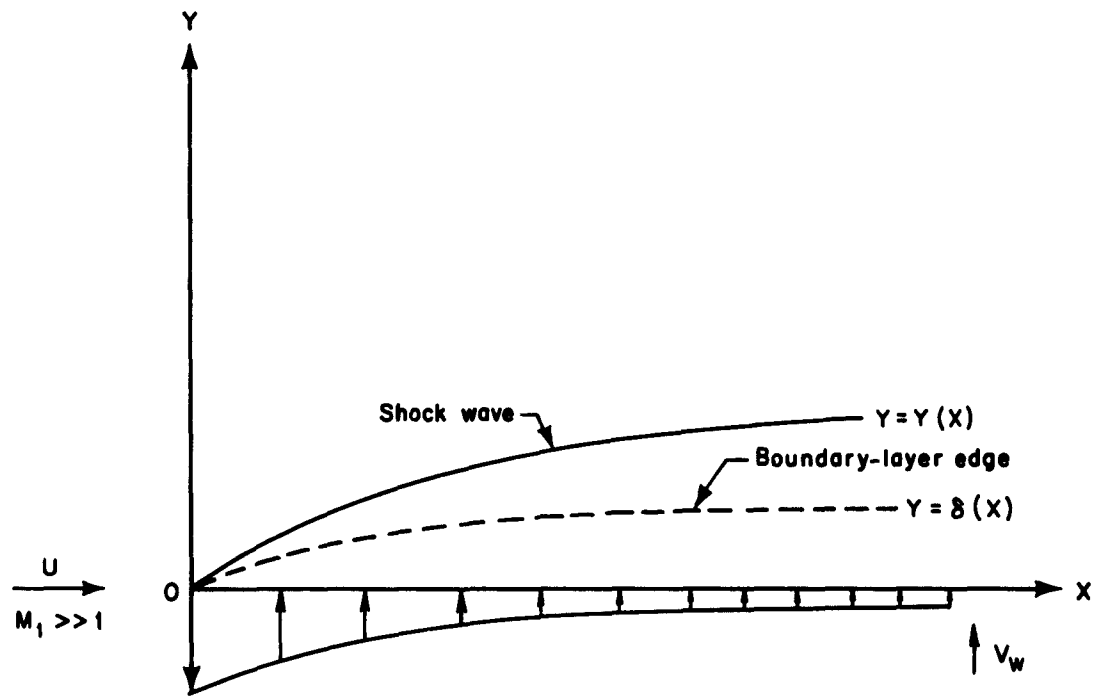


Fig. 1—Coordinate system and flat plate

$$\rho u \frac{\partial i}{\partial x} + \rho v \frac{\partial i}{\partial y} = u \frac{\partial p}{\partial x} + \mu \left(\frac{\partial u}{\partial y} \right)^2 + \frac{\partial}{\partial y} \left(k \frac{\partial T}{\partial y} \right) + v \frac{\partial p}{\partial y} \quad (5)$$

$$p = R\rho T \quad (6)$$

We assume that the fluid medium consists of a pure perfect gas with constant specific heat; therefore, $i = c_p T$. As stated in the Introduction, we regard these simplifying assumptions as acceptable for an initial attempt, and we shall consider the corrections to account for the imperfect-gas mixture behavior in a later section. Equation (2) is the continuity equation for the entire disturbed-flow region. Equation (3) is the boundary-layer equation applicable in the viscous region adjacent to the plate surface. In the inviscid-flow region, Eq. (3) becomes simply

$$\rho u \frac{\partial u}{\partial x} + \rho v \frac{\partial u}{\partial y} = - \frac{\partial p}{\partial x} \quad (3a)$$

Equation (4) is the y-momentum equation for the inviscid-flow region. In the boundary layer, Eq. (4) becomes, in the present approximate theory,

$$\frac{\partial p}{\partial y} = 0 \quad (4a)$$

Equation (5) is the energy equation for the disturbed-flow region. In the inviscid-flow region, Eq. (5) becomes simply

$$\rho u \frac{\partial i}{\partial x} + \rho v \frac{\partial i}{\partial y} = u \frac{\partial p}{\partial x} + v \frac{\partial p}{\partial y} \quad (5a)$$

In the boundary-layer region, Eq. (5) can be combined with Eq. (4a) to yield

$$\rho u \frac{\partial i}{\partial x} + \rho v \frac{\partial i}{\partial y} = u \frac{\partial p}{\partial x} + \mu \left(\frac{\partial u}{\partial y} \right)^2 + \frac{\partial}{\partial y} \left(k \frac{\partial T}{\partial y} \right) \quad (5b)$$

Equation (6) is the equation of state. Comparing Eqs. (2) and (5) with the Navier-Stokes equations, one finds that many terms in the Navier-Stokes equations are omitted in the present system. These omissions can be justified, in the range of x considered in Eq. (1), by the well-known order-of-magnitude arguments.

Our problem is to determine u , v , p , q , and T as functions of (x, y) which satisfy the following boundary conditions:

$$\begin{aligned} x > 0, \quad u(x, 0) = 0, \quad v(x, 0) = v_w(x) \\ T(x, 0) = T_w \end{aligned} \tag{7}$$

$$\begin{aligned} y \rightarrow \infty, \quad u(x, \infty) = U, \quad v(x, \infty) = 0 \\ p(x, \infty) = p_1, \quad \rho(x, \infty) = \rho_1, \quad T(x, \infty) = T_1 \end{aligned} \tag{8}$$

The conditions in Eq. (7) are specified at the plate surface which is assumed to have a uniform temperature T_w . The velocity of injection, which we shall specify later, is represented by $v_w(x)$. The conditions in Eq. (8) are the conditions of the undisturbed free stream; the subscript 1 is being used here to signify the free-stream conditions. We note that Eq. (8) also specifies the flow conditions for all y when $x < 0$.

III. THE INVISCID-FLOW REGION

The inviscid-flow region is governed by Eqs. (2), (3a), (4), (5a), and (6). This region is bounded by the leading-edge shock wave which separates it from the free stream. The shock-wave conditions may be expressed as

$$\frac{p_s}{p_1} = \frac{2\gamma}{\gamma + 1} M_1^2 \left(\frac{dY}{dx}\right)^2 - \frac{\gamma - 1}{\gamma + 1} \quad (9)$$

$$\frac{\rho_s}{\rho_1} = \frac{(\gamma + 1) M_1^2 \left(\frac{dY}{dx}\right)^2}{(\gamma - 1) M_1^2 \left(\frac{dY}{dx}\right)^2 + 2} \quad (10)$$

$$v_s = \frac{2}{\gamma + 1} \left(U \frac{dY}{dx} \right) \left[1 - \frac{1}{M_1^2 \left(\frac{dY}{dx}\right)^2} \right] \quad (11)$$

where $y = Y(x)$ represents the shock-wave equation. Equations (9) and (11) must be applied as the boundary conditions for the equations of the inviscid region. Solutions of the inviscid region have been obtained by Stewartson⁽⁶⁾ and Oguchi.⁽⁸⁾ As pointed out in Ref. 9, these inviscid solutions are directly applicable in the present investigation.* In fact, the direct effects of the mass transfer at the plate surface are to modify the boundary-layer flow, and the inviscid-flow region is only influenced indirectly (through the matching between the inviscid- and viscous-flow regions).

In the development of our theory, we shall use Oguchi's inviscid solution in the matching procedure. We therefore briefly discuss here Oguchi's

*In Ref. 9, this interesting point is demonstrated by an order-of-magnitude analysis. The same kind of analysis can be put forward here.

inviscid solution. We have, from thermodynamics

$$di = Tds + \frac{dp}{\rho}$$

where s is the specific entropy. Hence, Eq. (5a) becomes

$$u \frac{\partial s}{\partial x} + v \frac{\partial s}{\partial y} = 0$$

For a perfect gas with constant specific heat, we have $s \propto \frac{p}{\rho^\gamma}$; hence

$$u \frac{\partial}{\partial x} \left(\frac{p}{\rho^\gamma} \right) + v \frac{\partial}{\partial y} \left(\frac{p}{\rho^\gamma} \right) = 0 \quad (5c)$$

Equations (2), (3a), (4), and (5c) form the exact system that determines u , v , p , and ρ in the inviscid region with the shock-wave conditions in Eqs. (9), (10), and (11). We introduce

$$\begin{aligned} x &= Lx^* \\ y &= Ley^* \\ u &= U \left[1 + \epsilon^2 u^*(x^*, y^*) \right] \\ v &= U\epsilon v^*(x^*, y^*) \\ p &= p_1 \gamma M_1^2 \epsilon^2 p^*(x^*, y^*) \\ \rho &= \rho_1 \rho^*(x^*, y^*) \end{aligned} \quad (12)$$

Where L is a characteristic length, ϵ is nondimensional, and $\epsilon^2 \ll 1$.

In Eq. (12), the starred quantities are nondimensional and are all assumed to be of the same order of magnitude. Substitution of Eq. (12) into Eqs. (2), (3a),

*We may take $L = 1$ in the present Memorandum.

(4), and (5c) yields

$$\frac{\partial \rho^*}{\partial x^*} + \frac{\partial}{\partial y^*} (\rho^* v^*) = 0 \quad (13)$$

$$\frac{\partial u^*}{\partial x^*} + v^* \frac{\partial u^*}{\partial y^*} + \frac{1}{\rho^*} \frac{\partial \rho^*}{\partial x^*} = 0 \quad (14)$$

$$\frac{\partial v^*}{\partial x^*} + v^* \frac{\partial v^*}{\partial y^*} + \frac{1}{\rho^*} \frac{\partial \rho^*}{\partial y^*} = 0 \quad (15)$$

$$\frac{\partial}{\partial x^*} \left(\frac{p^*}{\rho^* \gamma} \right) + v^* \frac{\partial}{\partial y^*} \left(\frac{p^*}{\rho^* \gamma} \right) = 0 \quad (16)$$

Equations (13) to (16) are the equations of the hypersonic-small-perturbation theory.⁽¹⁰⁾ The shock-wave conditions in Eqs. (9) to (11) now become

$$p_s^* = \frac{2\gamma K_\epsilon^2 - (\gamma - 1)}{\gamma (\gamma + 1) K_\epsilon^2} \left(\frac{dy^*}{dx^*} \right)^2 \quad (9a)$$

$$\rho_s^* = \frac{(\gamma + 1) K_\epsilon^2}{(\gamma - 1) K_\epsilon^2 + 2} \quad (10a)$$

$$v_s^* = \frac{2 (K_\epsilon^2 - 1)}{(\gamma + 1) K_\epsilon^2} \left(\frac{dy^*}{dx^*} \right) \quad (11a)$$

In these equations we have

$$K_\epsilon^2 = M_1^2 \epsilon^2 \left(\frac{dy^*}{dx^*} \right)^2 \quad (17)$$

which is the inviscid-hypersonic-similarity parameter, $K_\epsilon^2 \gg 1$.

*We have discarded $O(\epsilon^2)$ terms.

A stream function is defined

$$\psi = \psi(x^*, y^*)$$

such that

$$\frac{\partial \psi}{\partial y^*} = \rho^* \quad \frac{\partial \psi}{\partial x^*} = -\rho^* v^* \quad (18)$$

Let $\frac{p^*}{\rho^* \gamma} = \omega^*$; then from Eq. (16) we have $\omega^* = \omega^*(\psi)$.

Equation (15) can be rewritten as

$$\begin{aligned} \left(\frac{\partial \psi}{\partial y^*}\right)^2 \frac{\partial^2 \psi}{\partial x^{*2}} - 2 \frac{\partial^2 \psi}{\partial x^* \partial y^*} \left(\frac{\partial \psi}{\partial x^*}\right) \frac{\partial \psi}{\partial y^*} + \left(\frac{\partial \psi}{\partial x^*}\right)^2 \frac{\partial^2 \psi}{\partial y^{*2}} \\ = \left(\frac{\partial \psi}{\partial y^*}\right)^{\gamma+1} \left\{ \gamma \omega^* \frac{\partial^2 \psi}{\partial y^{*2}} + \frac{d\omega^*}{d\psi} \left(\frac{\partial \psi}{\partial y^*}\right)^2 \right\} \end{aligned} \quad (18)$$

which is the differential equation for ψ . If the shock wave is expressed as

$$y^* = x^{*n} \quad 0 < n < 1 \quad (20)$$

then a similarity variable θ can be defined as

$$\theta = \frac{y^*}{x^{*n}} \quad (21)$$

and ψ can be expressed as

$$\psi(x^*, y^*) = x^{*n} f(\theta) \quad (22)$$

Substituting Eq. (22) into Eq. (19) yields

$$\begin{aligned} n^2 f'^2 f'' + n(n-1) (f - \theta f') (f')^2 \\ = \frac{2n}{\gamma+1} \left(\frac{\gamma-1}{\gamma+1}\right)^\gamma (f')^{\gamma+1} f^{\frac{2(n-1)}{n}} \left\{ n\gamma f'' + 2(n-1) \frac{f'^2}{f} \right\} \end{aligned} \quad (23)^*$$

In the shock wave conditions, we neglect $O\left(\frac{1}{k_e^2}\right)$ terms and thus obtain from Eqs. (9a), (10a), (11a), and (20)

* In Section III, the prime denotes differentiation with respect to θ .

$$f(1) = 1$$

$$f'(1) = \frac{\gamma + 1}{\gamma - 1} \quad (24)$$

The function $f(\theta)$ can be obtained from integration of Eq. (23) under the boundary conditions specified in Eq. (24). It should be noted that a singularity develops at the point $\theta = \theta_0$ where f vanishes. We let

$$f \sim A(\theta - \theta_0)^N \quad N > 0 \quad (25)^*$$

We then find that

$$p^* = \frac{2n^2}{\gamma + 1} \left(\frac{\gamma - 1}{\gamma + 1} \right)^\gamma x^* \frac{2(n-1)}{(f')^\gamma} f^{\frac{2n-1}{n}}$$

$$\sim (f')^\gamma f^{\frac{2(n-1)}{n}} \sim (\theta - \theta_0)^{\frac{2(n-1)}{n} N + (N-1)\gamma} \quad (26)$$

The pressure p^* is bounded and nonvanishing as $\theta \rightarrow \theta_0$, provided that

$$N = \frac{n\gamma}{2(n-1) + n\gamma} > 0 \quad (27)$$

For $\frac{2}{3} \geq \gamma > 1$, Eq. (27) implies that

$$1 > n > \frac{2}{3} \quad (27a)$$

For the strong-interaction region on a flat plate, we shall show $n = 3/4$ (see Eq. (60)). The constants A and θ_0 can be obtained from the following asymptotic values

$$A \sim \left(\frac{f'}{N} \right)^N f^{1-N}$$

$$\theta_0 \sim \theta - \frac{f}{f'} N \quad (28)$$

as $f \rightarrow 0$. These constants are readily evaluated from the solution of

*We are interested here in the leading term in f . In Ref. 8, the series expression of f has been given.

Eq. (23), using a stepwise integration starting from the shock wave. The integration can be carried out by using values of $f(1)$ and $f'(1)$ given in Eq. (24) to compute $f''(1)$ from Eq. (23). Further, Eq. (23) can be differentiated and used to compute $f'''(1)$, $f''''(1)$, etc. We then can determine

$$f(1 + \Delta h) = f(1) + \Delta h f'(1) + \frac{(\Delta h)^2}{2} f''(1) + \frac{(\Delta h)^3}{3} f'''(1) + \dots$$

Oguchi has carried out the calculations for $n = 3/4$ and $\gamma = 7/5$ (air) and $\gamma = 5/3$ (helium). These results are given as follows:

	A	θ_0
Air	4.40	0.591
Helium	2.44	0.479

Using Eqs. (25) and (18), we obtain

$$v_\delta^* = n x^{*n-1} \theta_0 \left[1 + 0 (\theta - \theta_0) \right] \quad (29)$$

By the definition in Eq. (12), we have, then, as $\theta \rightarrow \theta_0$

$$v_\delta = n \epsilon \left(\frac{x}{L} \right)^{n-1} \theta_0 U \quad (29a)$$

This gives the value of v_δ at the edge of the viscous boundary layer.

Equations (25) and (26) yield

$$p_\delta^* = \frac{2n^2}{\gamma + 1} \left(\frac{\gamma - 1}{\gamma + 1} \right)^\gamma (NA)^{\frac{1}{N}\gamma} (x^*)^{2(n-1)} \left\{ 1 + 0 (\theta - \theta_0)^N \right\} \quad (30)$$

Hence, for $\theta \rightarrow \theta_0$

$$p_\delta = \frac{2n^2}{\gamma + 1} \left(\frac{\gamma - 1}{\gamma + 1} \right)^\gamma \left[\frac{n\gamma}{2(n-1) + n\gamma} \right]^\gamma \left[A \right]^{\frac{n\gamma + 2(n-1)}{n}} \left(\frac{x}{L} \right)^{2(n-1)} \gamma M_1^2 p_1 \epsilon^2 \quad (30a)$$

This gives the pressure distribution in the boundary layer. Equations (29a) and (30a) provide the useful relations for matching the inviscid solution with the viscous-boundary-layer solution. We shall return to these relations later, but we shall now turn to the discussion of the viscous-flow region.

IV. THE VISCOUS-FLOW REGION

The viscous-flow region is governed by Eqs. (2), (3), (4a), (5b), and (6). The conditions at the plate surface are specified in Eq. (7). This viscous-flow region must possess a solution that can be smoothly joined to the inviscid solution described in the previous section. In fact, Eqs. (29a) and (30a) give the values of v_δ and p_δ at the edge of the boundary layer. It is noted that Eq. (29a) specifies that $v_\delta = O(\epsilon)$. This normal velocity is, physically speaking, the outward-flow velocity that accounts for the boundary-layer-displacement effect. In other words, as far as the boundary-layer calculations are concerned, the inviscid stream is parallel to the plate surface. This main flow is displaced outward by the boundary-layer effects which produce the value of v_δ . Hence, in the boundary-layer calculations, the leading terms of the inviscid-stream conditions are

$$\rho_\delta u_\delta \frac{du_\delta}{dx} = - \frac{dp_\delta}{dx} \quad (31a)$$

$$\rho_\delta \frac{di_\delta}{dx} = \frac{dp_\delta}{dx} \quad (31b)$$

$$p_\delta(x) = R \rho_\delta(x) T_\delta(x) \quad (31c)$$

These conditions are obtainable from the inviscid-flow equations for a main stream parallel to the plate surface.

In boundary-layer calculations, it is convenient to introduce

$$H = 1 + \frac{1}{2} u^2 \quad (32)$$

The values of H within the boundary layer must satisfy the equation

$$\rho u \frac{\partial H}{\partial x} + \rho v \frac{\partial H}{\partial y} = \frac{\partial}{\partial y} \left(\frac{\mu}{Pr} \frac{\partial H}{\partial y} \right) + \frac{\partial}{\partial y} \left[\mu \left(1 - \frac{1}{Pr} \right) \frac{\partial}{\partial y} \left(\frac{u^2}{2} \right) \right] \quad (33)$$

which is easily obtained by combining Eqs. (3) and (56). By Eq. (4a), within the boundary layer, we must have

$$\rho(x,y) T(x,y) = \rho_0(x) T_0(x) = \frac{1}{R} p_0(x) \quad (34)$$

Using this relation, we eliminate the variable ρ from Eqs. (2), (3), and (33) and thus obtain

$$\frac{\partial}{\partial x} \left(\frac{u}{T} \right) + \frac{\partial}{\partial y} \left(\frac{v}{T} \right) = - \frac{u}{T} \frac{1}{p_0} \frac{dp_0}{dx} \quad (35)$$

$$\frac{1}{T} \left(u \frac{\partial u}{\partial x} + v \frac{\partial u}{\partial y} \right) = - \frac{R}{p_0} \frac{dp_0}{dx} + \frac{R}{p_0} \frac{\partial}{\partial y} \left(\mu \frac{\partial u}{\partial y} \right) \quad (36)$$

$$\frac{1}{T} \left(u \frac{\partial H}{\partial x} + v \frac{\partial H}{\partial y} \right) = \frac{R}{p_0} \frac{\partial}{\partial y} \left(\frac{\mu}{Pr} \frac{\partial H}{\partial y} \right) + \frac{R}{p_0} \frac{\partial}{\partial y} \left\{ \left(1 - \frac{1}{Pr} \right) \mu \frac{\partial}{\partial y} \left(\frac{u^2}{2} \right) \right\} \quad (37)$$

In terms of these variables, Eq. (7) becomes

$$y = 0: u = 0, v = v_w(x), H = H_w = c_p T_w \quad (38)$$

which are the surface conditions. The main-stream boundary conditions are

$$y \rightarrow \infty: u \rightarrow u_0, H \rightarrow H_0 \quad (39)$$

From Eqs. (31a) and (31b) we easily obtain

$$H_0 = i_0 + \frac{1}{2} u_0^2 = \text{const.} \quad (40)$$

In a homenergetic flow, the constant term on the right-hand side of Eq.

(40) must be $H_1 = i_1 + \frac{1}{2} U^2$. Therefore, $H_0 = H_1$.

The next step in the boundary-layer calculations is the introduction of a stream function: (3)

$$\psi(x, y) = \int_0^y \frac{u}{R} dy + \psi_v(x) \quad (41)$$

Then we obtain

$$\frac{\partial \psi}{\partial y} = \frac{u}{R} \quad (42)$$

From Eq. (35), we also obtain

$$\frac{v}{R} = -\frac{1}{p_0} \frac{dp_0}{dx} \psi - \frac{\partial \psi}{\partial x} \quad (43)$$

$$\frac{v_v}{R} = -\frac{1}{p_0} \frac{dp_0}{dx} \psi_v - \left(\frac{\partial \psi}{\partial x} \right)_v \quad (44)$$

It is noted that Eqs. (42) and (43) can also be written as

$$\rho u = \frac{1}{R} \frac{\partial}{\partial y} (p_0 \psi) \quad (42a)$$

$$\rho v = -\frac{1}{R} \frac{\partial}{\partial x} (p_0 \psi) \quad (43a)$$

These expressions can be compared with the conventional stream function

$\bar{\psi}$ defined as follows:

$$\rho v = -\frac{\partial \bar{\psi}}{\partial x} \quad (45)$$

$$\rho u = \frac{\partial \bar{\psi}}{\partial y} \quad (46)$$

Thus we obtain

$$\bar{\psi} = \frac{1}{R} p_0 \psi \quad (47)$$

The streamlines can be obtained as lines of $\bar{V} = \frac{1}{R} p_0 \psi = \text{const.}$; ψ , which may be called the reduced stream function, is a generalization of the function used in Ref. 5.

Now, Eqs. (36) and (37) can be rewritten as

$$\frac{\partial \bar{V}}{\partial y} \frac{\partial u}{\partial x} - \left(\frac{1}{p_0} \frac{dp_0}{dx} \psi + \frac{\partial \bar{V}}{\partial x} \right) \frac{\partial u}{\partial y} = - \frac{R}{p_0} \left\{ \frac{dp_0}{dx} - \frac{\partial}{\partial y} \left(\mu \frac{\partial u}{\partial y} \right) \right\} \quad (36a)$$

$$\frac{\partial \bar{V}}{\partial y} \frac{\partial H}{\partial x} - \left(\frac{1}{p_0} \frac{dp_0}{dx} \psi + \frac{\partial \bar{V}}{\partial x} \right) \frac{\partial H}{\partial y} = \frac{R}{p_0} \left[\frac{\partial}{\partial y} \left(\frac{\mu}{Pr} \frac{\partial H}{\partial y} \right) + \frac{\partial}{\partial y} \left\{ \mu \left(1 - \frac{1}{Pr} \right) \frac{\partial}{\partial y} \left(\frac{u^2}{2} \right) \right\} \right] \quad (37a)$$

We let

$$\psi(x, y) = N(x) K(\eta) \quad (48)$$

$$u(x, y) = u_0(x) K'(\eta) \quad (49)^*$$

$$H(x, y) = H_1 G(\eta) \quad (50)$$

where η is the similarity variable for the boundary-layer flow. An explicit definition of η will be obtained later. Substitution of Eqs. (48), (49), and (50) into Eqs. (36a) and (37a) yields, after some manipulations,

$$\left(K'^2 - \frac{R}{Pr} \right) \frac{\frac{1}{u_0} \frac{du_0}{dx}}{\frac{1}{p_0 N} \frac{d(p_0 N)}{dx}} - KK'' = R^2 \frac{Cp_0 \mu_0 u_0}{p_0 N \frac{d(p_0 N)}{dx}} (\lambda K'')' \quad (36b)$$

$$\frac{1}{p_0 N} \frac{d(p_0 N)}{dx} KG' = \left(\frac{R}{p_0 N} \right)^2 Cp_0 \mu_0 u_0 \left[\left(\frac{\lambda G'}{Pr} \right)' + \frac{u_0^2}{H_1} \left\{ \left(1 - \frac{1}{Pr} \right) \lambda K' K'' \right\}' \right] \quad (37b)$$

where the parameter

$$\lambda = \frac{1}{C} \frac{\rho \mu}{p_0 \mu_0} \quad (51)$$

*In Section IV, the prime denotes differentiation with respect to η .

has been introduced after Baron,⁽¹¹⁾ and C is the Chapman-Rubens constant.⁽¹²⁾ We now let

$$s = \left(\frac{1}{\sqrt{2}} \frac{p_0 H}{R} \right)^2 = C \int_0^x \rho_0 u_0 u_0' dx \quad (52)$$

Then Eqs. (36b) and (37b) may be expressed as

$$(\lambda K'')' + K K'' - \frac{2s}{u_0} \frac{du_0}{ds} (K'^2 - \frac{T}{T_0}) = 0 \quad (36c)$$

$$K G' + \left(\frac{\lambda G'}{Pr} \right)' + \frac{u_0^2}{H_1} \left[\left(1 - \frac{1}{Pr} \right) \lambda K' K'' \right]' = 0 \quad (37c)$$

The above calculations are simple extensions of the method of Ref. 5. Equations (36b) and (37b) can also be obtained by following different approaches such as those used in Refs. 7 and 11. Using Eq. (32) we can rewrite the last group of terms in Eq. (36c) as

$$\frac{2s}{u_0} \frac{du_0}{ds} (K'^2 - \frac{T}{T_0}) = - \frac{H_0}{H_0 - \frac{1}{2} u_0^2} \cdot \frac{p_0}{\rho_0 u_0^2} \cdot \frac{(K'^2 - G)}{1 + \frac{\frac{1}{H} \frac{dH}{dx}}{\frac{1}{p_0} \frac{dp_0}{dx}}} \quad (53)$$

The conditions at the edge of the boundary layer give

$$\frac{u_0^2}{H_0} = \frac{2}{1 + \frac{2}{\gamma - 1} \frac{1}{M_0^2}}$$

$$\frac{p_0}{\rho_0 u_0^2} = \frac{1}{\gamma M_0^2}$$

Thus, Eq. (53) can be rewritten as

$$\frac{2s}{u_0} \frac{du_0}{ds} \left(K'^2 - \frac{T}{T_0} \right) = - \frac{\gamma - 1}{2\gamma} \left(1 + \frac{2}{\gamma - 1} \cdot \frac{1}{M_0^2} \right) \frac{K'^2 - G}{1 + \frac{\frac{1}{N} \frac{dN}{dx}}{\frac{1}{P_0} \frac{dP_0}{dx}}} \quad (53a)$$

For $M_0^2 \gg 1$, we thus obtain

$$\frac{2s}{u_0} \frac{du_0}{ds} \left(K'^2 - \frac{T}{T_0} \right) \approx - \frac{\gamma - 1}{2\gamma} \frac{(K'^2 - G)}{1 + \frac{\frac{1}{N} \frac{dN}{dx}}{\frac{1}{P_0} \frac{dP_0}{dx}}} \quad (53b)$$

The right-hand-side expression is a function of η only, provided that

$$\frac{\frac{1}{N} \frac{dN}{dx}}{\frac{1}{P_0} \frac{dP_0}{dx}} = m = \text{const.} \quad (54)$$

Therefore, in order to obtain the similar solutions of the boundary layer we must have

$$N \sim P_0^m \quad (55)$$

From Eq. (52), it then follows that

$$C_{p_0} \mu_0 u_0 \sim P_0^{2m+1} \frac{dP_0}{dx} \quad (52a)$$

But

$$C_{p_0} \mu_0 u_0 \sim \frac{P_0}{T_0} T_0 u_0$$

$$- p_0 \left[H_0 \left(1 - \frac{1}{1 + \frac{2}{\gamma - 1} \frac{1}{M_0^2}} \right) \right]^{\omega - 1} \left(\frac{2H_0}{1 + \frac{2}{\gamma - 1} \frac{1}{M_0^2}} \right)^{1/2} - p_0$$

Thus, Eq. (52a) implies that

$$p_0^{2m} \frac{dp_0}{dx} = \text{const.} \quad (52b)$$

whence we have

$$p_0 \sim x^{\frac{1}{2m+1}} \quad (56)$$

Now, from Eq. (43), we have

$$\begin{aligned} \frac{v_0}{T_0} &\sim -\frac{1}{p_0} \frac{dp_0}{dx} \quad v_0 \sim -\frac{1}{p_0} \frac{dp_0}{dx} N(x) K(\infty) \\ &\sim p_0^{m-1} \frac{dp_0}{dx} \sim x^{2(n-1)(m-1) + (2n-3)} \end{aligned} \quad (57)$$

Comparing Eqs. (29a) and (57), we obtain

$$2(m-1) + \frac{2n-3}{n-1} = 1 \quad (58)$$

Comparing Eqs. (30a) and (56), we obtain

$$2(n-1) = \frac{1}{2m+1} \quad (59)$$

Equations (58) and (59) are used to determine the values of n and m ;

thus, we have

$$n = \frac{3}{4}, \quad m = -\frac{3}{2} \quad (60)$$

These values of n and m are necessary to permit the matching of the inviscid solution of Section III with the viscous solution of the present section. We shall discuss the matching procedure in a later section. By

Eqs. (53b) and (54), now, we obtain

$$\frac{2s}{u_0} \frac{du_0}{ds} (K'^2 - \frac{T}{T_0}) = + \frac{\gamma-1}{\gamma} (K'^2 - G) \quad (53c)$$

Therefore, in the hypersonic-strong-interaction region on a flat plate, Eqs. (36c) and (37c) can be written as

$$(\lambda K'')' + K K'' = \frac{\gamma-1}{\gamma} (K'^2 - G) \quad (36d)$$

$$K G' + \left(\frac{\lambda G'}{Pr} \right)' + 2 \left[\left(1 - \frac{1}{Pr} \right) \lambda K' K'' \right]' = 0 \quad (37d)$$

where terms of $O(\frac{1}{M_0^2})$ are neglected because $M_0^2 \gg 1$. Equations (36d) and (37d) can be used to compute the similar solutions $K(\eta)$ and $G(\eta)$. The boundary conditions in Eqs. (38) and (39) yield the following conditions:

$$\eta \rightarrow 0 \quad K' = 0, \quad K = \text{const.}, \quad G = \frac{H_W}{H_1} = \frac{T_W}{T_0} \quad (38a)$$

$$\eta \rightarrow \infty \quad K' = 1, \quad G = 1 \quad (39a)$$

where T_0 denotes the stagnation temperature of the undisturbed free stream. The condition $K(0) = \text{const.}$ implies a particular value of $v_w(x)$ that will be discussed in the next section. We note here that the similarity variable η is related as

$$\eta = \frac{\rho_0 u_0}{\sqrt{2s}} \int_0^y \frac{\rho}{\rho_0} dy \quad (61)$$

This result can be easily obtained from Eqs. (34), (42), (49), and (52). Equation (61) shows that the similarity variable used here is the same one adopted in Ref. 11.

A great simplification of the system of equations derived above can be achieved by taking $Pr = 1$, $\omega = 1$. In this simplified case, we obtain

$$\begin{aligned}
 K''' + KK'' &= \beta(K'^2 - G) \\
 KG' + G'' &= 0 \\
 \eta \rightarrow 0 : K' &= 0, \quad K = \text{const.}, \quad G = \frac{T_s}{T_\infty} \\
 \eta \rightarrow \infty : K' &= 1, \quad G = 1
 \end{aligned} \tag{62}$$

where

$$\beta = \frac{\gamma - 1}{\gamma}$$

To obtain a preliminary estimate of the mass-transfer effects on the strong-interaction phenomena on a flat plate, numerical integration of this simplified system has been carried out for $\gamma = 7/5$ and $\gamma = 5/3$. Results are summarized in Figs. 2 through 12. In these numerical results, $G(0)$ and $K(0)$ have been assigned the following ranges of values:

$$G(0) = \frac{T_s}{T_\infty} = 0, 0.5, 0.99, 2.0, 4.0, 6.0, 8.0, 10.0$$

$$K(0) = 0, \pm 0.2, \pm 0.4, \pm 0.6$$

For $Pr = 1$, $G(0) = 1$ corresponds to the case of an insulated surface, and $G(0) < 1$ corresponds to the case of a cooled surface. Positive values of $K(0)$ represent suction ($v_w < 0$), and negative values of $K(0)$ represent injection ($v_w > 0$) (see Eq. (68a), next section). Also calculated are values of I and $I^{1/2}$ where I is defined as

$$I = \int_0^\infty (G - K'^2) d\eta \tag{63}$$

We shall use these values of I in later calculations. In practice, the upper limit of integration in Eq. (63) is finite, its value η_0 being given in Figs. 2 through 12 also.

V. THE LAW OF SURFACE MASS TRANSFER FOR SIMILAR SOLUTIONS

In deriving the equations and boundary conditions for the similar solutions in the boundary-layer flow, it has been necessary to take $K(0) = \text{const.}$ In this section, we briefly discuss the significance of this condition. We obtain, from Eqs. (48) and (44),

$$K(0) = \frac{1}{\Gamma(x) N(x)} \frac{v_w}{T_w} \quad (64)$$

where $N(x)$ has been defined in Eq. (48), and

$$\Gamma(x) = - \frac{1}{p_s N} \frac{d}{dx} (p_s N) \quad (65)$$

In the present investigation, T_w is assumed constant. Therefore, in order that $K(0) = \text{const.}$, we must have

$$v_w = C_1 \Gamma(x) N(x) \quad C_1 = T_w K(0) \quad (66)$$

where C_1 is a constant. Equation (66) gives the law of injection necessary for similar solutions. For $\omega = 1$, we obtain

$$v_w = - \frac{C_1}{\sqrt{\frac{4}{k}}} \sqrt{\frac{R \mu_1 U}{T_1}} p_0^{1/4} x^{-1/4} \quad (67)$$

where it has been assumed that $p_s = (p_0 x)^{-1/2}$, p_0 being a constant to be determined later (Eq. (72)). This is the law of injection for similar solutions in the hypersonic-strong-interaction region of a flat plate. It follows, from Eq. (67), that

$$\frac{\rho_w v_w}{\rho_1 U} = - \frac{K(0)}{\sqrt{\frac{4}{k}}} \sqrt{\frac{p_0}{p_1}} \frac{v_1}{U} p_0^{3/2} \quad (68)$$

In Ref. 4, Yasuhara used the conditions $v_w \propto x^{-1/4}$ and $\frac{\rho_w v_w}{\rho_1 U} \propto p_0^{3/2}$ which are in agreement with Eqs. (67) and (68). The present theory therefore contains Yasuhara's results as a special case, namely, the case of an insulated plate. Equation (68) can be rewritten as

$$K(0) = -2 \frac{\rho_w v_w}{\rho_1 U} \sqrt{\frac{Ux}{v_1} \left(\frac{p_1}{p_0}\right)^{1/2}} = K_0 \quad (68a)$$

This shows that for $K(0) = \text{const.}$ the mass-transfer rate at the plate surface must follow the special law in Eq. (68a). If a transpiration-cooling system is to be designed based on this analysis, then a particular arrangement of pumps, storage tanks, pressure regulators, and accessories is needed to produce this special mass-transfer rate. In the case of a film-cooling system or a sublimation- or ablation-cooling system, some further studies are necessary to obtain an idea of the feasibility of this special surface-mass-transfer rate.

VI. MATCHING OF THE INVISCID- AND VISCOUS-FLOW SOLUTIONS

The complete solution of the strong-interaction region on the flat plate will be discussed in the present section. The viscous-boundary-layer solution must be matched to the inviscid solution. Such a matching can be carried out in one of the following three schemes:

1. Scheme I: The inviscid solution due to Oguchi⁽⁸⁾ is matched to the viscous-boundary-layer solution.
2. Scheme II: The inviscid solution due to Stewartson⁽⁶⁾ is matched to the viscous-boundary-layer solution.
3. Scheme III:⁽¹³⁾ The inviscid solution is approximately represented by the tangent-wedge approximation and is then matched to the viscous-boundary-layer solution.

We shall discuss briefly here Scheme I, making use of the results obtained in Sections III and IV. In carrying out this scheme of matching between the viscous and inviscid solutions, we shall adopt the simplifications $Pr = 1$, $\omega = 1$.

From Eq. (61), we obtain

$$\delta = (\gamma - 1) M_1^2 \sqrt{\frac{v_1}{U}} \left(\frac{p_1}{p_0} \right)^{1/4} x^{3/4} \int_0^{\infty} (G - K^2) d\eta \quad (69)$$

From Eqs. (45) and (46), on the streamline $\psi = \text{const.}$, we have

$$\frac{v}{u} = - \frac{\partial \psi / \partial x}{\partial \psi / \partial y} = - \left(\frac{dy}{dx} \right)_{\psi}$$

whence, by Eq. (47), we have

$$\frac{y}{u} = - \frac{\frac{\partial}{\partial \eta} (P_0 \psi)}{\frac{\partial}{\partial \eta} (P_0 \psi)} = \frac{dy}{dx} \quad (70)$$

It follows that

$$\frac{v_0}{U} = \frac{dy}{dx} = \frac{3}{4} (\gamma - 1) M_1^2 \sqrt{\frac{v_1}{U}} \sqrt{P_1 P_0}^{1/4} x^{-1/4} \int_0^{\eta} (G - K^2) d\eta \quad (70a)$$

where δ has been determined from Eq. (69). Equation (70a) can be compared with Eq. (29a);* thus we obtain

$$L^{1/4} \epsilon = (\gamma - 1) M_1^2 \sqrt{\frac{v_1}{U}} \sqrt{\frac{P_1 P_0}{\theta_0}}^{1/4} I \quad (71)$$

where I is the integral defined in Eq. (63). To determine ϵ from Eq. (71), we need to know P_0 which, by Eqs. (30a),* can be given as

$$P_0 = \left[\frac{9\gamma}{8(\gamma+1)} \left\{ \frac{(\gamma-1)}{(\gamma+1)} \frac{1}{(1-\frac{2}{3\gamma})} \right\}^{\gamma} \Lambda^{\gamma-\frac{2}{3}} L^{1/2} M_1^2 P_1 \epsilon^2 \right]^{-2} \quad (72)$$

It follows that

$$\sqrt{P_1 P_0}^{1/4} = \left[\frac{9\gamma}{8(\gamma+1)} \left\{ \frac{\gamma-1}{(\gamma+1)} \frac{1}{(1-\frac{2}{3\gamma})} \right\}^{\gamma} \Lambda^{\gamma-\frac{2}{3}} \right]^{-1/2} \frac{1}{M_1 (\epsilon L^{1/4})} \quad (72a)$$

*In Eqs. (29a) and (30a), we take $n = 3/4$ (see Eq. (60)).

Combining Eqs. (71) and (72a), we obtain

$$\epsilon = \left\{ (\gamma - 1) \frac{I}{\theta_0} \right\}^{1/2} \left[\frac{8(\gamma + 1)}{9\gamma} \left\{ \frac{(\gamma + 1)(1 - \frac{2}{3\gamma})}{(\gamma - 1)} \right\}^\gamma A^{2/3 - \gamma} \right]^{1/4} \sqrt{M_1} \sqrt{\frac{v_1}{Ux}} \quad (71a)$$

Finally, we obtain here a definition of the nondimensional parameter ϵ .

Substituting ϵ from Eq. (71a) into Eq. (30a) yields

$$\frac{P_0}{P_1} = \left[\frac{9\gamma}{8(\gamma + 1)} \left\{ \frac{\gamma - 1}{(\gamma + 1)(1 - \frac{2}{3\gamma})} \right\}^\gamma A^{\gamma - 2/3} \right]^{1/2} \frac{(\gamma - 1) I}{\theta_0} \left\{ M_1^3 \sqrt{\frac{v_1}{Ux}} \right\} \quad (73)$$

Equation (73) gives the pressure distribution in the strong-interaction region on the plate surface. For $\gamma = 1.4$, $\theta_0 = 0.591$, and $A = 4.40$, we obtain, from Eq. (73),

$$\frac{P_0}{P_1} = .4248 \quad I \left\{ M_1^3 \sqrt{\frac{v_1}{Ux}} \right\} \quad (73a)$$

Combining Eqs. (69), (72a), and (71a), we obtain

$$M_1 \frac{\delta}{x} = \left[\frac{8(\gamma + 1)}{9\gamma} \left\{ \frac{(\gamma + 1)(1 - \frac{2}{3\gamma})}{\gamma - 1} \right\}^\gamma A^{2/3 - \gamma} \right]^{1/4} \sqrt{(\gamma - 1)\theta_0} \sqrt{I} \left(M_1^3 \sqrt{\frac{v_1}{Ux}} \right)^{1/2} \quad (74)$$

Equation (74) gives the boundary-layer-thickness distribution in the strong-interaction region on the plate surface. For $\gamma = 1.4$, we obtain, from Eq. (74),

$$M_1 \frac{\delta}{x} = 0.615 \sqrt{I} \left\{ M_1^3 \sqrt{\frac{v_1}{Ux}} \right\}^{1/2} \quad (74a)$$

To obtain the surface shearing stress, $\tau = (\mu \frac{\partial u}{\partial y})_w$, we have from Eq. (49)

$$\tau = \frac{\mu_w U^2 K''(0)}{N T_w} \quad (75)$$

The local-skin-friction coefficient is then defined as

$$c_{f_1} = \frac{\tau}{\frac{1}{2} \rho_1 U^2}$$

which can be expressed as

$$\frac{1}{\sqrt{C}} c_{f_1} \sqrt{\frac{Ux}{v_1}} = \left(\frac{\gamma - 1}{\theta_0} \right)^{1/2} \left[\frac{9\gamma}{8(\gamma + 1)} \left\{ \frac{\gamma - 1}{(\gamma + 1)(1 - \frac{2}{3\gamma})} \right\}^\gamma A^{\gamma - \frac{2}{3}} \right]^{1/4} \sqrt{I} \left\{ M_1^3 \sqrt{\frac{v_1}{Ux}} \right\}^{1/2} K''(0) \quad (76)$$

This gives the variation of the skin-friction coefficient in the strong-interaction region on the plate surface. For $\gamma = 1.4$, we have

$$\frac{1}{\sqrt{C}} c_{f_1} \sqrt{\frac{Ux}{v_1}} = (.4248 I)^{1/2} K''(0) \left(M_1^3 \sqrt{\frac{v_1}{Ux}} \right)^{1/2} \quad (76a)$$

We define the local heat-transfer coefficient c_{h_1} as

$$c_{h_1} = \frac{-k_w \left(\frac{\partial T}{\partial y} \right)_w}{\rho_1 U H_1 [G(0) - 1]}$$

We then find that

$$\frac{c_{h_1}^2}{c_{f_1}} = \frac{-1}{G(0) - 1} \frac{G'(0)}{K''(0)} \quad (77)$$

Equations (73), (74), (76), and (77) are the results of matching the inviscid and viscous solutions by Scheme I. In these calculations, we have used the simplification $Pr = 1$ and $\omega = 1$. In the matching procedure, the viscous-boundary-layer solution has been joined continuously with Oguchi's inviscid solution regarding flow variables, including pressure and normal velocity. No attempt has been made here to join continuously the inviscid and viscous solutions regarding the temperature and density. To make the matching consistent regarding temperature and density, a higher-approximation theory similar to Oguchi's theory in Ref. 8 must be developed. In such a higher-approximation theory it can be anticipated that the interaction between surface mass transfer and the entropy layer behind the shock wave will produce interesting effects. The treatment of the higher-approximation theory will be deferred to a future report, and the discussion will be confined to the present approximation theory. It will be seen that important effects due to surface mass transfer can be found within the present theory.

VII. RESULTS AND DISCUSSION

BOUNDARY-LAYER THICKNESS

Figure 2 shows the effect of mass transfer and wall temperature on the boundary-layer thickness. The mass-transfer behavior is quite similar to that experienced by a noninteracting boundary layer. The boundary-layer thickness increases when material is injected and decreases when material is removed by suction at the wall. The wall-temperature variation of the boundary-layer thickness shows an interesting property. The results indicate that the boundary-layer thickness is most insensitive to mass-transfer effects for hot- and cold-wall conditions. The percentage change in thickness at a given injection or suction rate increases to a maximum value which is reached at $T_w/T_o = 1$. This percentage change then decreases until it is reduced to less than the cold-wall ($T_w/T_o = 0$) value. This would indicate that the boundary layer is most "malleable" at $T_w/T_o = 1$, as far as the boundary-layer thickness (and, of course, induced wall pressure) is concerned. This is the point at which the mass transfer affects the coupled boundary layer most effectively.

INDUCED SURFACE PRESSURE

Figure 3 shows the variation of the induced pressure at the wall with mass transfer and wall temperature. Since the boundary-layer thickness and induced pressure are directly related, the behavior of the two are quite similar. The induced wall pressure increases with surface injection because of the thickening boundary layer. Suction at the wall produces the opposite effect. The induced pressure exhibits the same maximum sensitivity at $T_w/T_o = 1$.

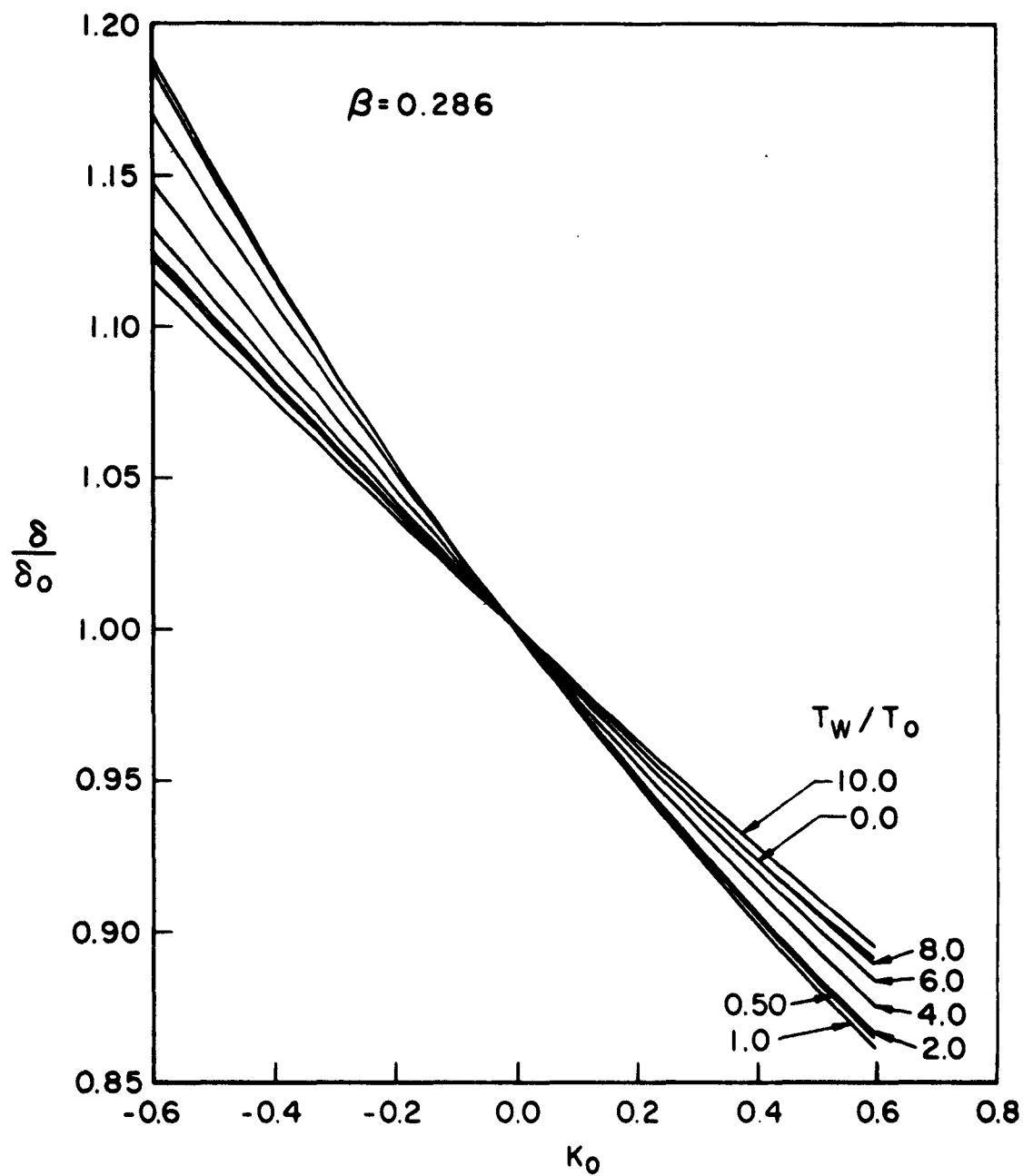


Fig. 2 — Influence of mass transfer on boundary-layer thickness

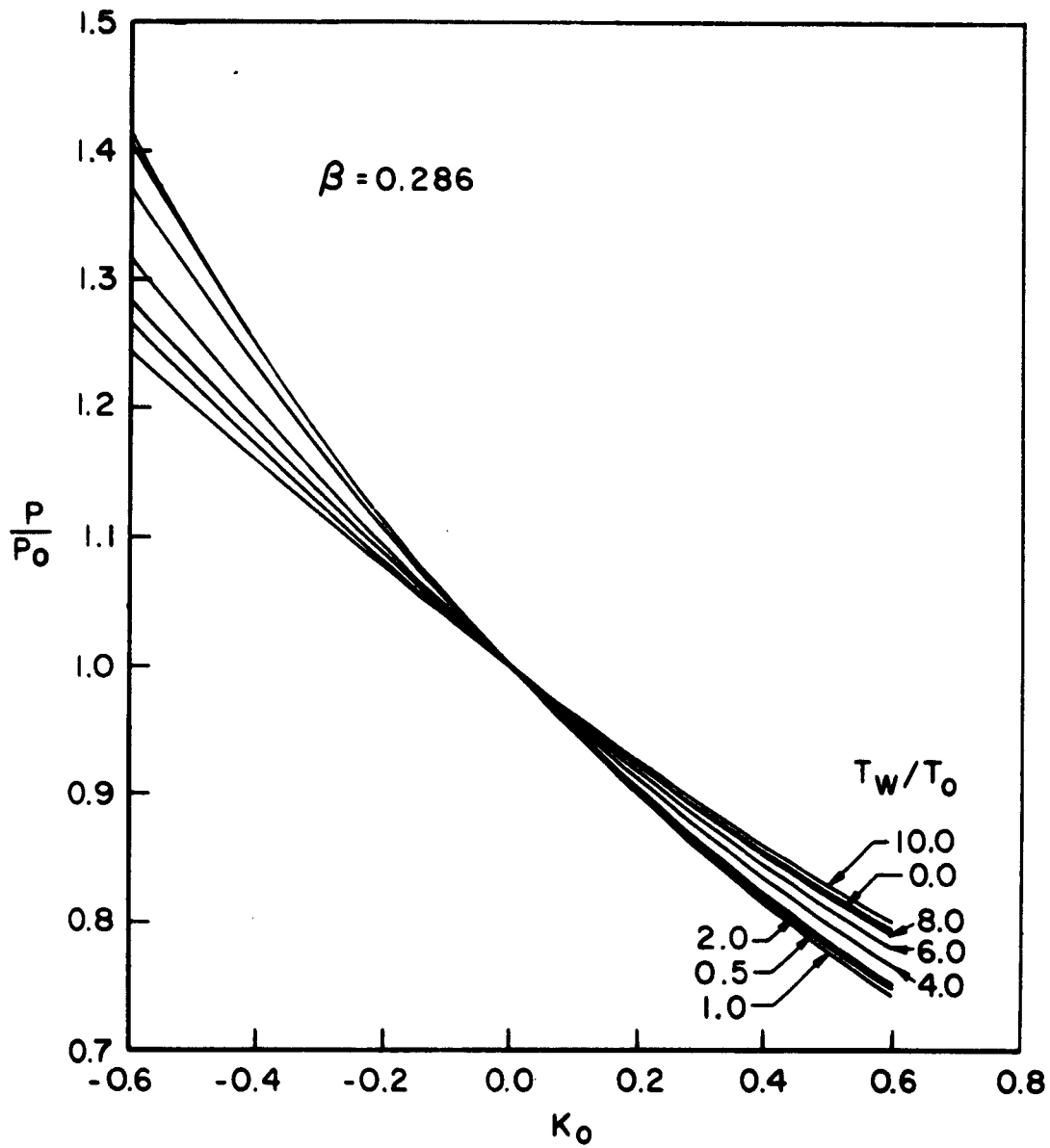


Fig. 3 — Influence of mass transfer on induced surface pressure

VELOCITY PROFILES

The velocity profiles in an interacting viscous boundary layer show some unusual characteristics with varying mass transfer and wall temperature. This behavior effects an interesting variation in the skin-friction coefficient. When the temperature of the wall is low ($T_w/T_o < 2$) (see Fig. 4), the velocity profiles respond to wall injection and suction in the usual manner; that is, the velocity gradient at the wall increases, and the profile becomes more shallow as mass is removed from the boundary layer. It can be seen how the boundary-layer thickness is decreased. The opposite effects are brought about by injection.

As the wall temperature is increased ($T_w/T_o > 4.0$), several things begin to happen (see Fig. 5). First, the velocity profile at the wall becomes more independent of the mass-transfer parameter K_o until (at $T_w/T_o > 8.0$) (Fig. 6) it is a constant for all values of K_o representing extremes of wall suction and injection. Second, the velocity gradient increases generally with the increase in wall temperature, finally approaching a limit at $T_w/T_o \sim 8.0$. The interesting thing to note is that the wall velocity gradient and the boundary-layer thickness do not behave in a similar fashion. The reason for this is the appearance at moderate wall temperatures ($T_w/T_o = 4.0$) of a local velocity overshoot at about the middle of the boundary layer. Since the pressure is constant throughout the boundary layer, this overshoot is caused by the acceleration of low-density material near the wall. This effect was first observed by Li and Nagamatsu⁽²⁾ for the solid-wall case at a similar temperature and a $\beta = 0.400$. The effect here is much greater because higher wall temperatures have been investigated. The effect appears for the first time at $T_w/T_o = 4.0$. The overshoot is small (1 to 2 per cent),

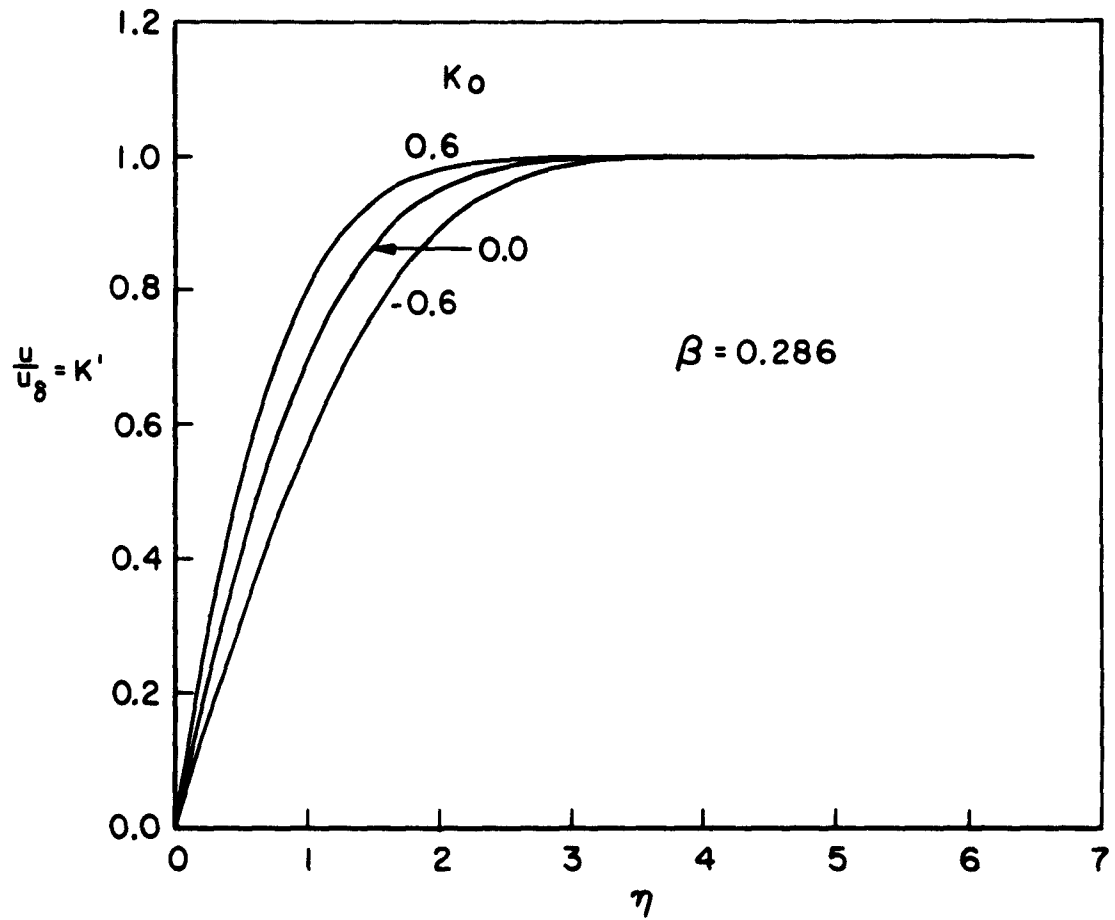


Fig.4—Influence of mass transfer on velocity profiles in the boundary layer for $T_w/T_0 = 2.0$

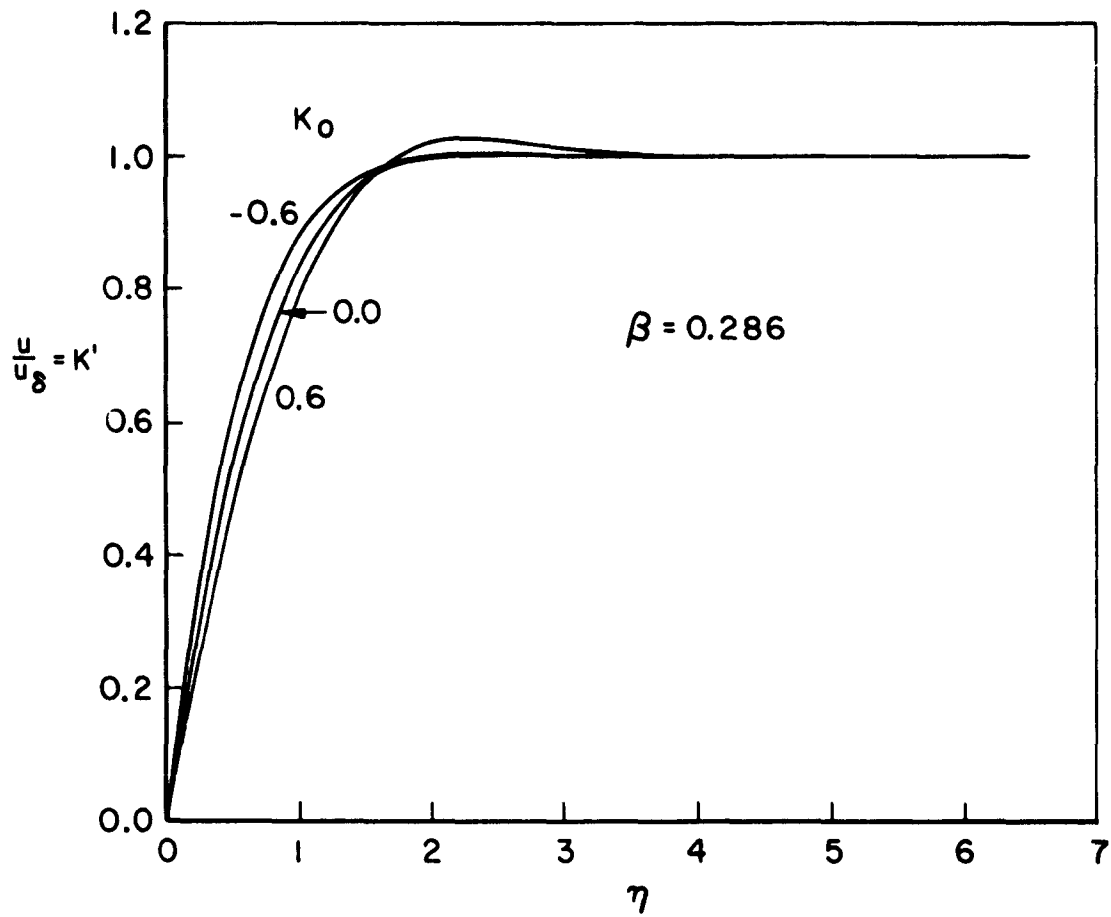


Fig. 5 — Influence of mass transfer on velocity profiles in the boundary layer for $T_w/T_0 = 4.0$

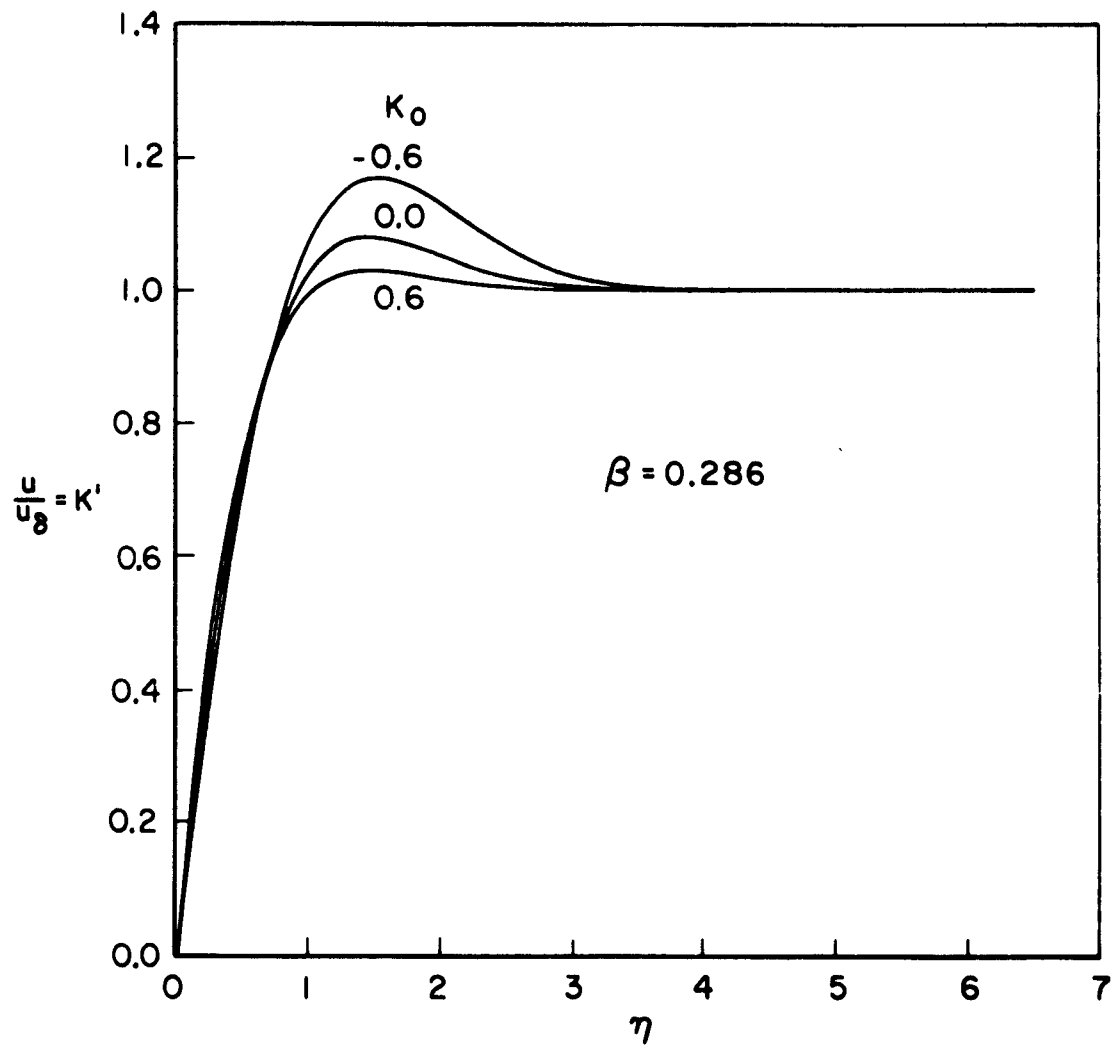


Fig. 6 — Influence of mass transfer on velocity profiles in the boundary layer ($T_w/T_0 = 8.0$)

and the wall mass-transfer condition still influences the slope of the velocity profile rather than the height of the overshoot. As the wall temperature increases, the mass-transfer parameter K_0 no longer affects the wall velocity gradient, but rather changes the maximum value of the velocity overshoot in the boundary layer. At high wall temperature ($T_w/T_0 = 10$, $\beta = 0.286$) the overshoot at high injection ($K_0 = -0.6$) can be 25 per cent higher than the velocity at the outer edge of the boundary layer. The fact that the surface mass transfer changes only the overshoot values and not the wall gradient explains the interesting result that the skin-friction coefficient is insensitive to variation of mass transfer for very-hot-wall conditions, as can be seen in Fig. 10. In fact, for $T_w/T_0 = 10$, both injection and suction decrease the skin-friction coefficient, albeit by a small amount.

TEMPERATURE PROFILES

The thermal boundary layer is more regular in its behavior with mass transfer and wall temperature (see Fig. 7). The thermal boundary layer is about as thick as the dynamic boundary layer ($3.0 < \eta < 4.0$) and remains essentially constant in thickness as the wall-temperature ratio is increased. Although the temperature gradient at the wall becomes very large for the hot-wall case, it does not lose its sensitivity to the wall mass transfer (Fig. 8). It is still possible to change the heat transfer by significant amounts (50 per cent) even at very hot surfaces. There is no appearance of an overshoot similar to that in the velocity profile. Examination of Fig. 9 shows that adiabatic-wall cases above $T_w/T_0 = 4.0$ will be difficult to obtain with reasonable mass-transfer parameters. It is obvious that an enormous $K_0 < 0$ will be required to bring about an adiabatic wall condition. The boundary layer will have separated, invalidating the equations long before the proper

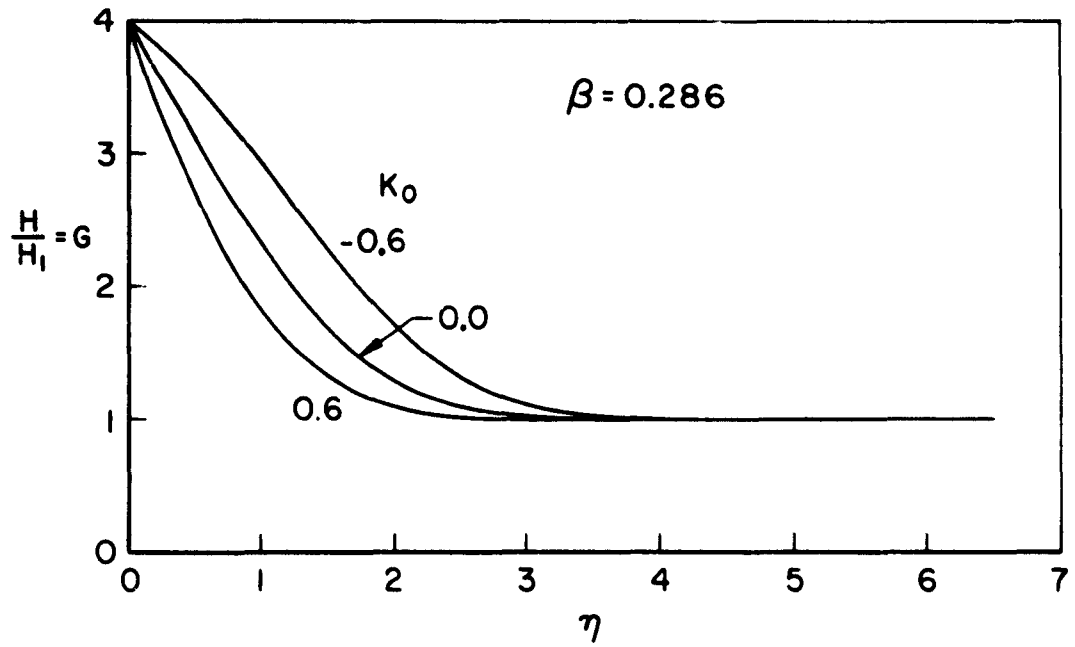


Fig.7—Influence of mass transfer on temperature profiles in the boundary layer ($T_w/T_0 = 4.0$)

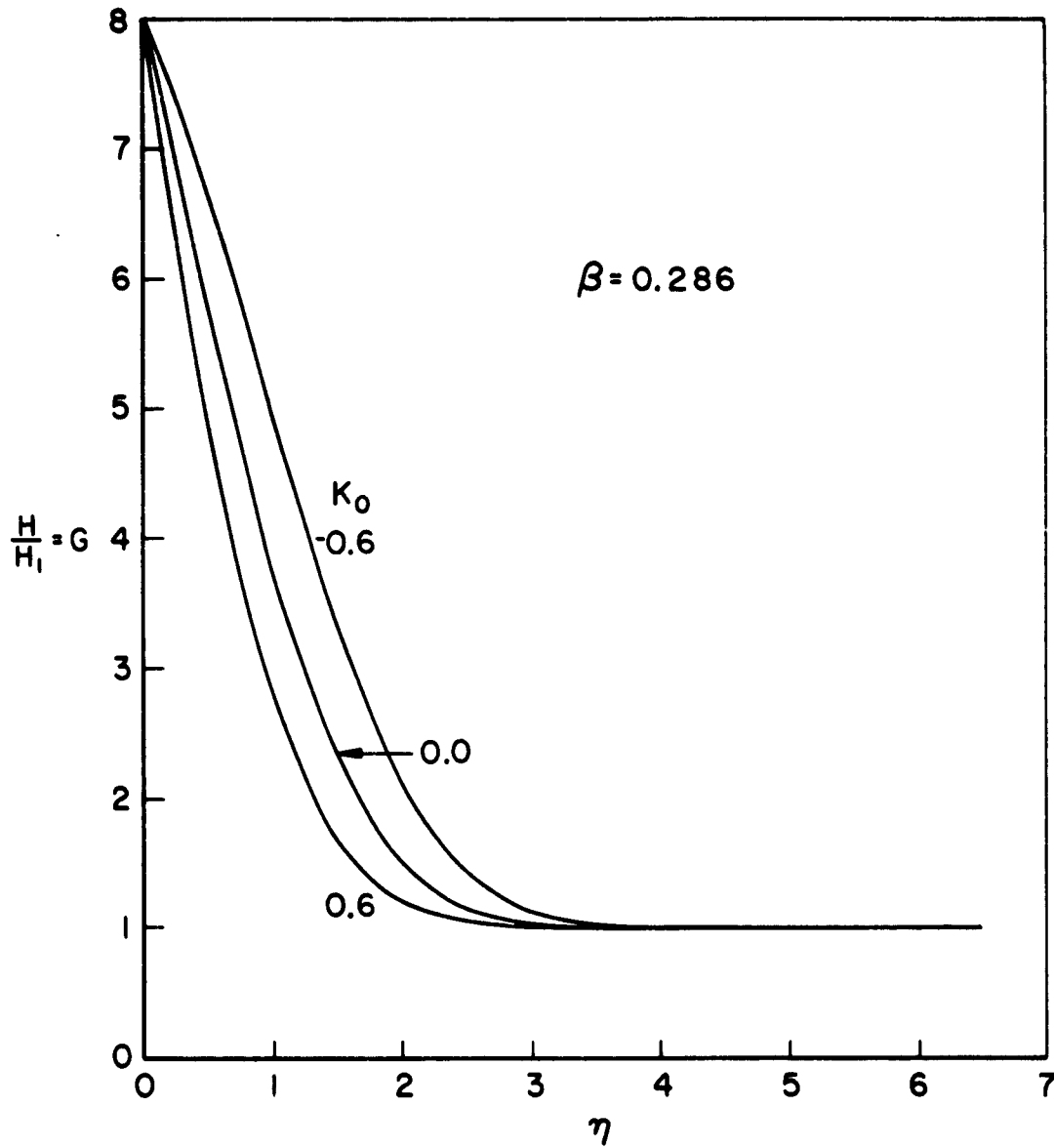


Fig. 8 —Influence of mass transfer on temperature profiles in the boundary layer ($T_w/T_0=8.0$)

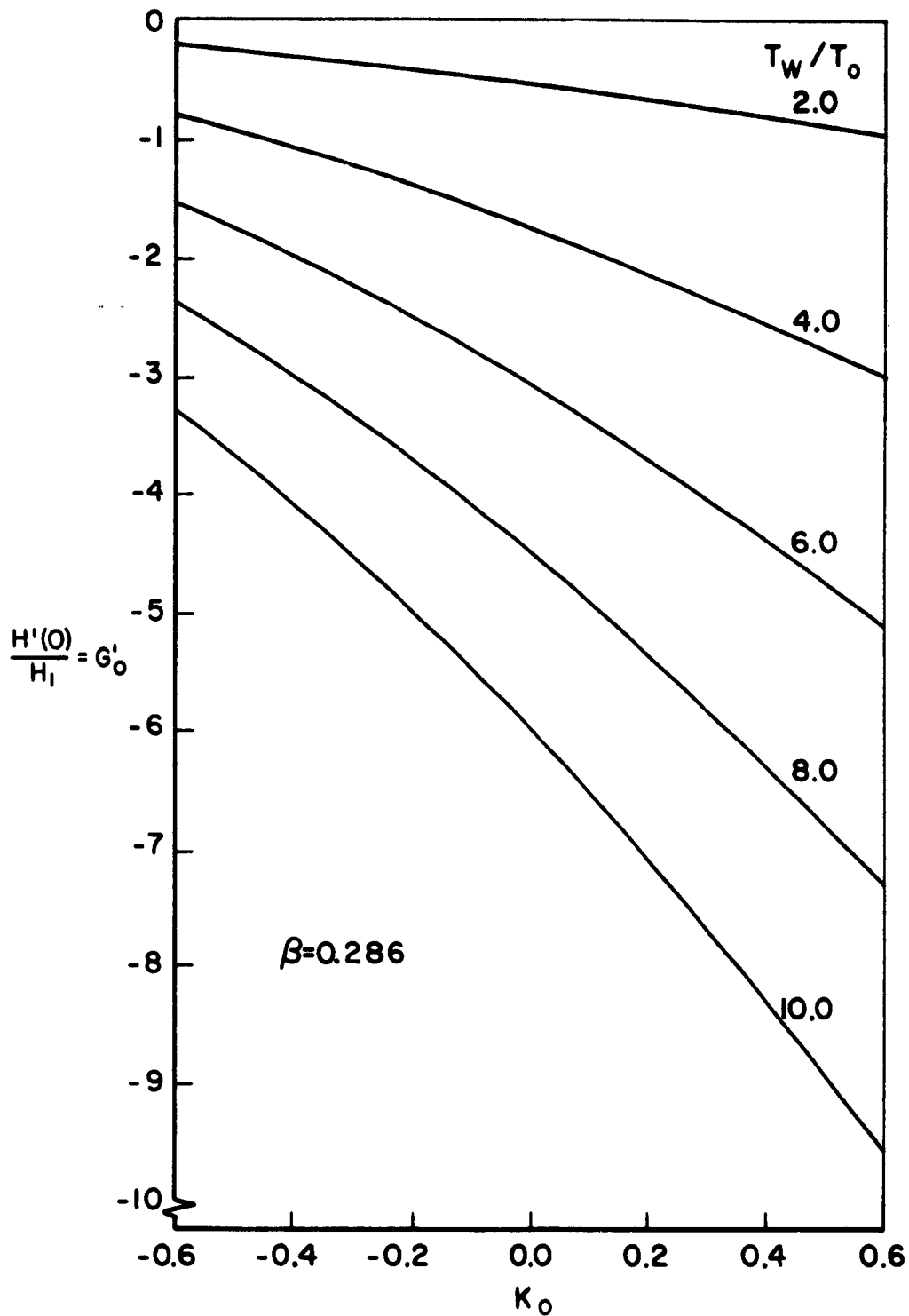


Fig. 9 —The influence of the wall temperature on the relationship between the heat and mass transfer at the wall

value is reached. It should prove interesting to see how these values respond to a higher pressure gradient.

SKIN-FRICTION COEFFICIENT

The variation of the skin-friction coefficient with mass transfer and wall temperature is shown in Fig. 10. The skin friction is most sensitive to mass transfer at a cold wall and loses this sensitivity quite rapidly as the wall temperature is increased. For $T_w/T_o > 6.0$, the skin-friction coefficient is essentially independent of mass transfer. The constancy of the skin-friction coefficient is a direct result of the insensitivity of the velocity gradient to mass transfer. Figure 10 illustrates the importance of mass-transfer cooling at low wall temperatures. It is interesting to note the linear character of the relationships. The skin-friction-coefficient variation can be described quite well by an equation of the form

$$\frac{c_f}{c_{f_o}} = 1 + A \left(\frac{T_w}{T_o} \right) K_o$$

HEAT-TRANSFER COEFFICIENT

The heat-transfer coefficient is shown in Fig. 11. It is much less sensitive to the wall temperature and retains its dependence on the mass transfer even at $T_w/T_o = 10.0$. This behavior is quite in line with the results obtained for the temperature profiles. Again the linearity of the mass-transfer dependence is noted. The heat-transfer coefficient may be described by

$$\frac{c_h}{c_{h_o}} = 1 + B \left(\frac{T_w}{T_o} \right) K_o$$

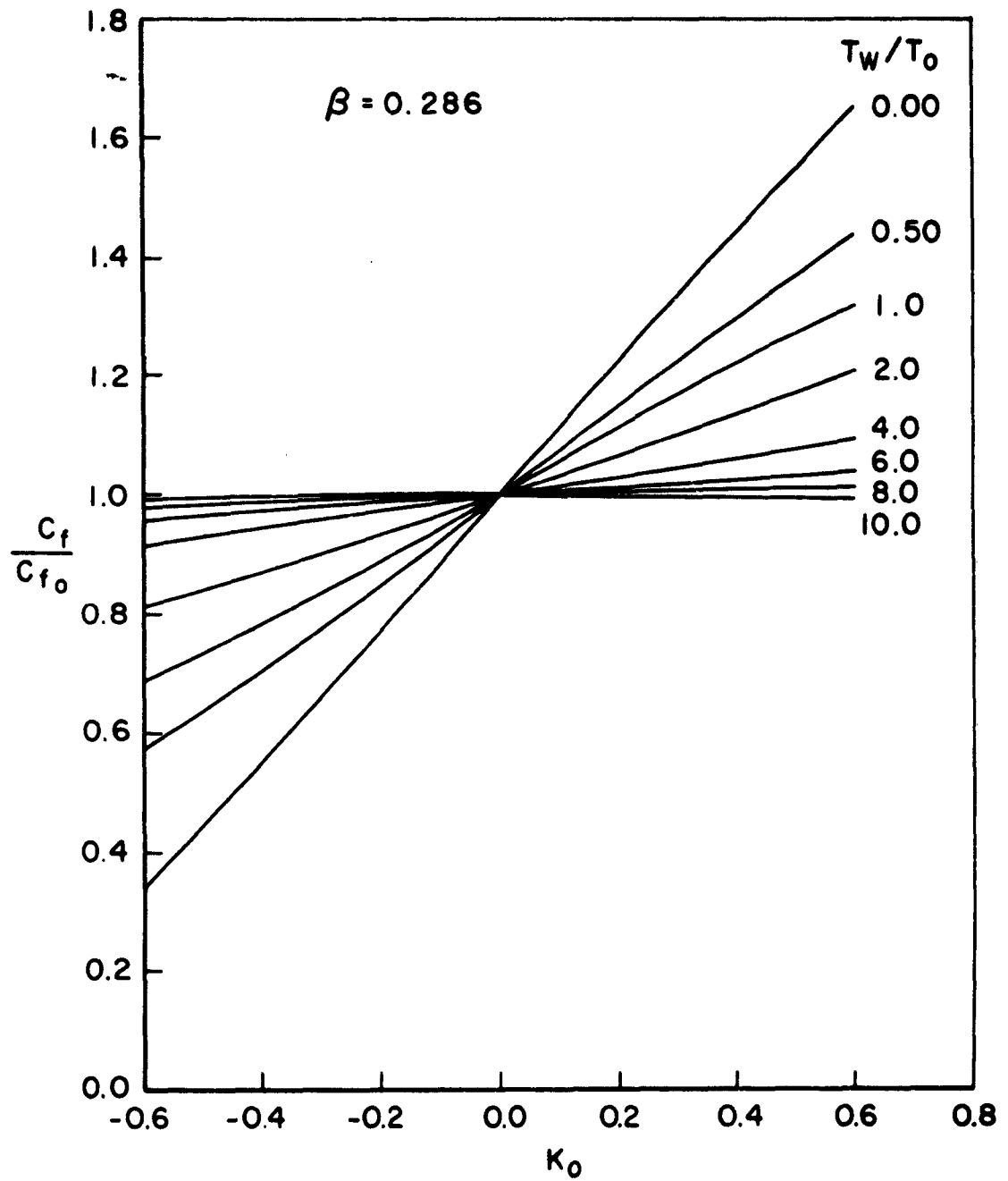


Fig.10—Influence of mass transfer on local skin-friction coefficient

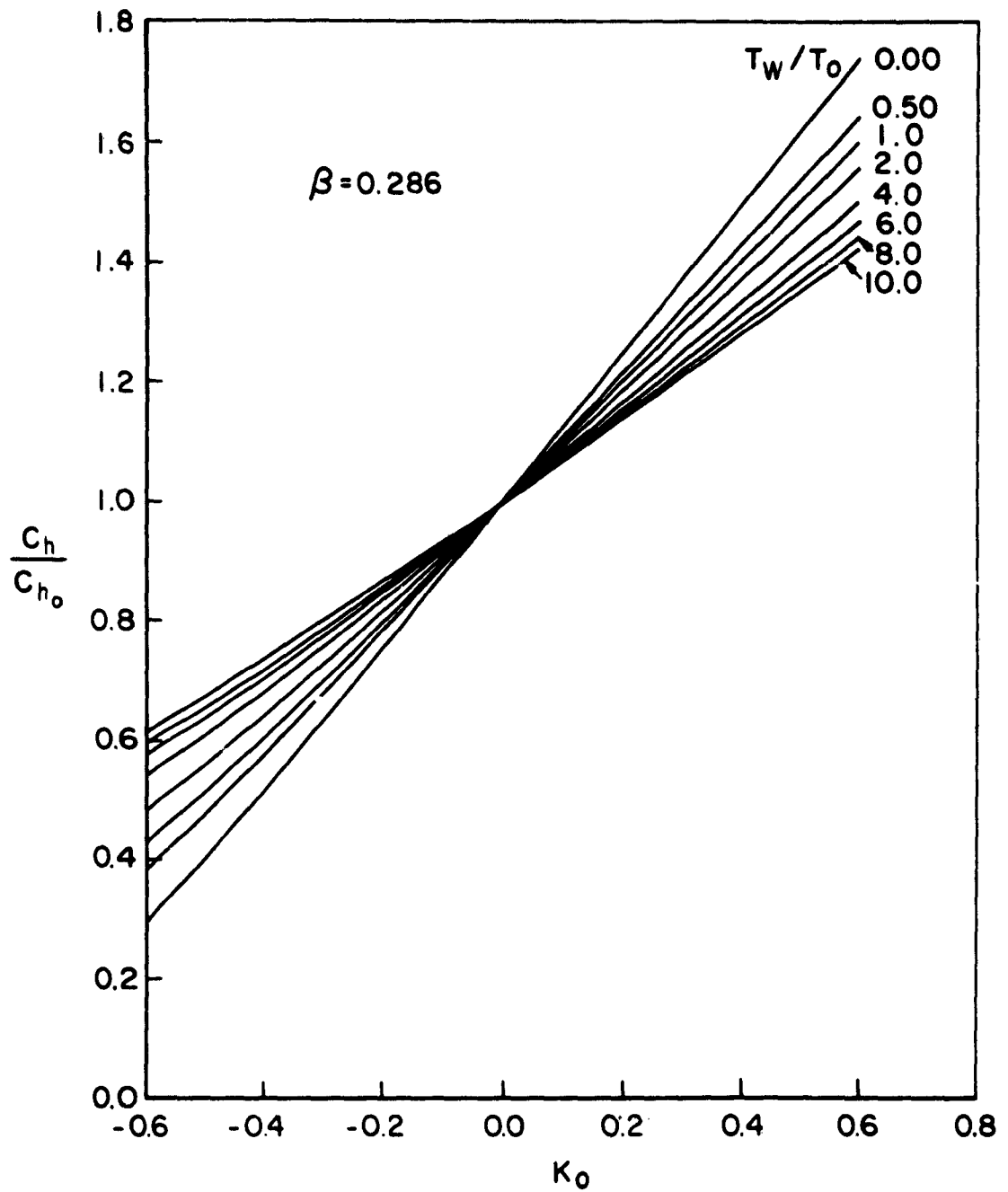


Fig.11—Influence of mass transfer on local heat-transfer coefficient

REYNOLDS ANALOGY

The different behavior of the velocity and temperature profiles at high wall temperatures would indicate severe deviations from the Reynolds analogy. This is shown in Fig. 12. From this it is possible to conclude that the Reynolds analogy is a reasonable approximation only for a cold wall; this approximation works better for suction than for injection.

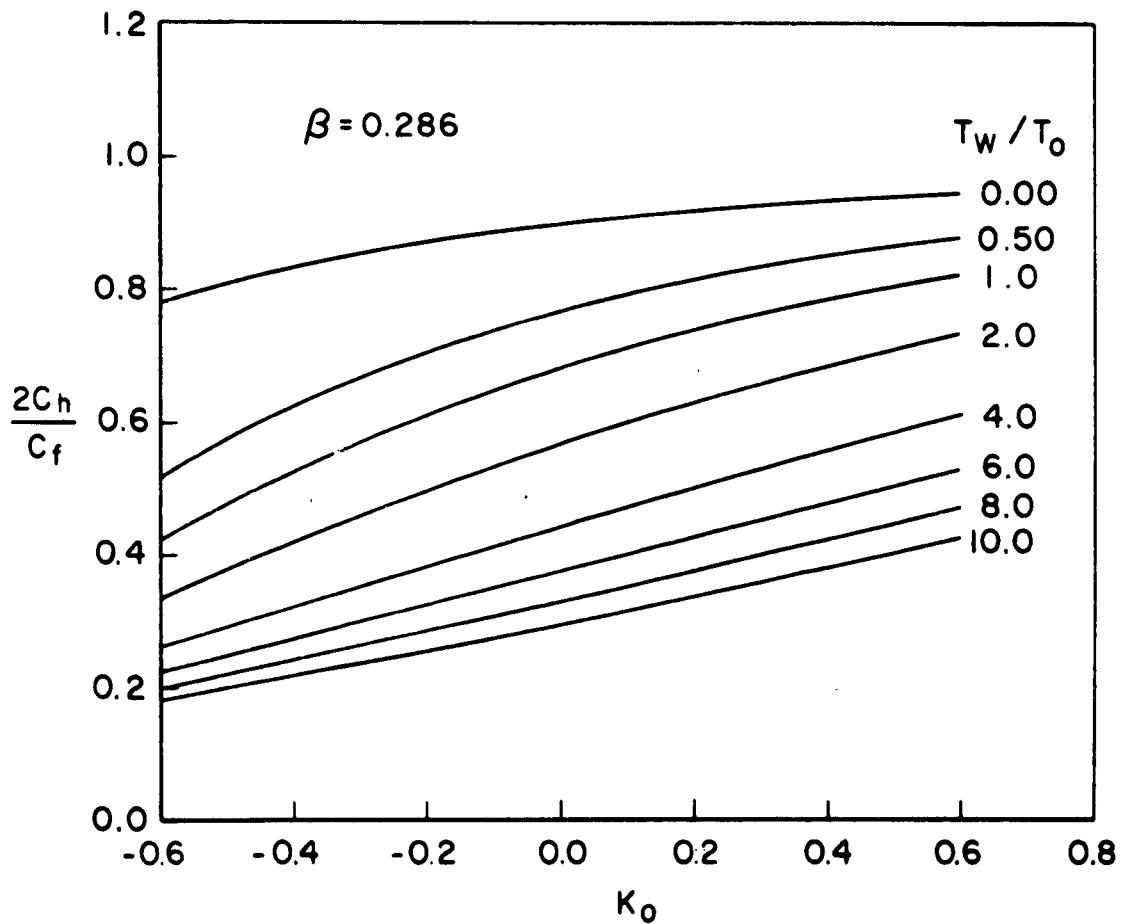


Fig 12—Influence of mass transfer on Reynolds' analogy

VIII. CONCLUDING REMARKS

The results of this study may be succinctly stated as follows:

1. The boundary layer thickens with injection, so that the interaction phenomena increase.
2. The percentage increase in the boundary-layer thickness is a function of the wall temperature and reaches a maximum when the ratio $T_w/T_0 = 1$.
3. The velocity and temperature profiles behave quite differently.
4. The velocity profiles exhibit an overshoot at high wall temperatures ($T_w/T_0 > 4$). The value of this overshoot, as well as the boundary-layer thickness, is dependent on the mass-transfer parameter, whereas the wall gradient is essentially a constant. This explains the constancy of the skin-friction coefficient with K_0 at high T_w/T_0 .
5. The temperature profiles retain their sensitivity to K_0 up to (and probably beyond) $T_w/T_0 = 10$. In order to achieve adiabatic wall conditions at high T_w/T_0 , values of K_0 will necessarily be so high that the boundary-layer equations will no longer be valid.
6. The Reynolds analogy breaks down for $T_w/T_0 > 0$. It retains its validity longer for suction than for injection.
7. Both the dimensionless skin-friction coefficient and heat-transfer coefficient exhibit remarkably linear behavior. It appears that over a broad range of parameters ($0 < T_w/T_0 < 10$; $-0.6 < K_0 < 0.6$) the coefficients may be expressed in the form

$$\frac{c_f}{c_{f_0}} = 1 + A \left(\frac{T_w}{T_0} \right) K_0$$

$$\frac{c_h}{c_{h_0}} = 1 + B \left(\frac{T_w}{T_0} \right) K_0$$

The analysis presented here is being extended in several directions:

1. The relationship of β to the other variables is being examined; all cases for $\beta = 0.400$ are being evaluated.*
2. The adiabatic wall condition is being examined.
3. The simple sublimation case is now being evaluated. This model is generated by requiring the Clausius-Clapeyron equation to be satisfied at the wall.

* These results have been presented in a paper ("Der Effekt der Druckverteilung auf die Stärke Zähigkeitswechselwirkung im Hyperschallgebiet an einer Platte mit Stoff-Austausch") read before the Wissenschaftliche Gesellschaft für Luftfahrt, Freiburg/Br., October 21, 1961.

REFERENCES

1. Gross, J. F., D. J. Masson, and C. Gazley, Jr., General Characteristics of Binary Boundary Layers With Applications to Sublimation Cooling, The RAND Corporation, P-1371, August 1, 1958.
2. Lees, L., Convective Heat Transfer With Mass Addition and Chemical Reactions, Combustion and Propulsion, Third AGARD Colloquium, Palermo, Sicily, March 1958.
3. Li, T. Y., Similar Solutions of Compressible Laminar-Boundary-Layer Equations for Binary Mixtures, The RAND Corporation, RM-2523 (ASTIA No. AD 238095), March 9, 1960.
4. Yasuhara, M., "On the Hypersonic Viscous Flow Past a Flat Plate With Suction or Injection," J. Phys. Soc. Japan, Vol. 12, No. 2, February 1957.
5. Li, T. Y., and H. T. Nagamatsu, "Similar Solutions of Compressible Boundary Layer Equations," 1954 Heat Transfer and Fluid Mechanics Institute, University of California; also J. Aero. Sci., Vol. 22, No. 9, September 1955, p. 607.
6. Stewartson, K., "On the Motion of a Flat Plate at High Speed in a Viscous Compressible Fluid--II, Steady Motion," J. Aero. Sci., Vol. 22, 1955, pp. 303-309.
7. Hayes, W. D., and R. F. Probstein, Hypersonic Flow Theory, Academic Press, New York, 1959.
8. Oguchi, H., First-Order Approach to a Strong Interaction Problem in Hypersonic Flow Over an Insulated Flat Plate, Aeronautical Research Institute, University of Tokyo, Report 330, June 1958.
9. Li, T. Y., Effect of Surface Mass-Transfer on the Hypersonic Strong Interaction Between Shock Wave and Boundary Layer, ARS Preprint No. 1144-60, May 1960.
10. Van Dyke, M. D., A Study of Hypersonic Small-Disturbance Theory, NACA Report 1194, 1954.
11. Baron, J. R., "The Heterogeneous Laminar Boundary Layer," in D. J. Masson (comp.), Mass-Transfer Cooling for Hypersonic Flight (U), The RAND Corporation, S-51 (ASTIA No. AD 133006), June 24, 1957 (Secret).
12. Chapman, D. R., and M. Rubesin, "Temperature and Velocity Profiles in the Compressible Laminar Boundary Layer With Arbitrary Distribution of Surface Temperatures," J. Aero. Sci., Vol. 16, No. 9, 1949, p. 547.
13. Li, T. Y., and H. T. Nagamatsu, "Hypersonic Viscous Flow on Noninsulated Flat Plate," Proc. 4th Midwestern Conf. on Fluid Mech., Purdue University, 1955, pp. 273-287.